Proceedings of the ASME 2010 3rd Joint US-European Fluids Engineering Summer Meeting and
8th International Conference on Nanochannels, Microchannels, and Minichannels
FEDSM-ICNMM2010
August 1-5, 2010, Montreal, Canada

FEDSM-ICNMM2010-30495

MEASUREMENT OF THE TIME DELAY ASSOCIATED WITH FLUID DAMPING CONTROLLED INSTABILITY IN A NORMAL TRIANGULAR TUBE ARRAY

John Mahon *
School of Engineering
Trinity College Dublin
Dublin, Ireland
Email: mahonjp@tcd.ie

Craig Meskell
School of Engineering
Trinity College Dublin
Dublin, Ireland
Email: cmeskell@tcd.ie

ABSTRACT

Fluidelastic instability produces large amplitude self-excited vibrations close to the natural frequency of the structure. It is now recognised as the excitation mechanism with the greatest potential for causing damage in tube arrays. It can be split into two mechanisms: fluid stiffness controlled and fluid damping controlled instability. The former is reasonably well understood, although a better understanding for fluid damping controlled instability is required. There is a time delay between tube motion and the resulting fluid forces at the root of fluid damping controlled instability. The exact nature of the time delay is still unclear. The current study directly measures the time delay between tube motion and the resulting fluid forces in a normal triangular tube array with a pitch ratio of 1.32 with air cross-flow. The instrumented cylinder has 36 pressure taps with a diameter of 1 mm, located at the mid-span of the cylinder. The instrumented cylinder was forced to oscillate in the lift direction at four excitation frequencies for a range of flow velocities. Unsteady pressure measurements at a sample frequency of 2kHz were simultaneously acquired along with the tube motion which was monitored using an accelerometer. The instantaneous fluid forces were obtained by integrating the surface pressure data. A time delay between tube motion and resulting fluid forces was obtained. The time delay measured was of the order of magnitude assumed in the semi-empirical models of by Price & Paidoussis (1984, 1986), Weaver and Lever et al.(1982, 1986, 1989, 1993), Granger & Paidoussis (1996), Meskell (2009), i.e. $t = \mu d/U$, with μ=O(1). Although, further work is required to provide a parameterized model of the time delay which can be embedded in these models, the data already provides some insight into the physical mechanism responsible.

NOMENCLATURE

c_s	Damping
c_{sp}	Speed of sound
C_D	Drag coefficient
C_L	Lift coefficient
C_P	Mean pressure coefficient
d	Tube diameter
F_D	Drag force
F_L	Lift force
E	Fluidelastic force
f_n	Natural frequency
FEI	Fluidelastic instability
k_s	Stiffness
l	Tube length
M_s	Mass
NT	Normal triangular
P	Pressure
P/d	Pitch ratio
P_θ	Mean pressure at a give position angle
$P_{\theta max}$	Mean pressure at stagnation point
Re	Reynolds number
U	Free stream flow velocity

*Address all correspondence to this author.

U_g	Gap velocity
U_r	Reduced velocity
$\dot{y}$	Tube displacement
$\dot{y}$	Tube velocity
$\ddot{y}$	Tube acceleration
y/d	Non-dimensional tube displacement
θ	Position angle
τ	Time delay
τ_1	Non-dimensional time delay (=τf)
τ_2	Non-dimensional time delay (=τU/d)
ε	System offset (Time delay)
ρ	Fluid density (air)

INTRODUCTION

Heat exchanger tube arrays are susceptible to damage due to flow-induced vibration, as they are typically long, slender structures with thin walls to promote heat transfer. There are several mechanisms responsible for flow-induced vibration, but fluidelastic instability is potentially the most destructive. Indeed, the stability threshold represents a design and operational limitation for many large scale heat exchangers and steam generators. For example, Adobes et al. (1) demonstrated that the fluidelastic critical velocity is the limiting factor for power output in a nuclear steam generator during stretch out operation.

Fluidelastic instability is characterized by a rapid increase in vibration amplitude as cross flow velocity is increased. It is well known that even a single flexible cylinder in a rigid tube bundle subject to cross flow may experience large amplitude self excited vibration referred to as fluidelastic instability (FEI). The subject of fluidelastic instability in tube arrays and models available for the phenomenon, have been reviewed in some detail by Price (2) and Paidoussis (3).

Chen (4; 5) examined the instability mechanisms and the stability criteria based on a previously developed mathematical model. His analysis resulted in the formulation of two instability mechanisms; fluid damping controlled instability and fluid stiffness controlled instability. The existence of two distinct mechanisms was also later shown by Price & Paidoussis (6). Experimental validation of the existence of two vibration mechanisms did not occur until the early ‘90s. Price & Kuran (7) using a rotated square array with P/d = 2.12 reported a minimum of three flexible cylinders for fluidelastic instability to occur. This demonstrated the existence of the fluid stiffness controlled mechanism which requires fluid coupling between adjacent cylinders (multiple degrees of freedom).

The nature of the time delay between tube motion and the resulting fluid forces at the root of fluid damping controlled instability is unclear. Granger & Paidoussis (8) indirectly measured the cause of the time delay using experimental data and a quasi-unsteady model. Meskell (9) developed a theoretical model for the memory function in the quasi-unsteady model. Abd-Rabbo & Weaver (10) conducted a flow visualisation on rotated square array with pitch ratio 1.41 and water cross-flow. For a single flexible cylinder flow visualisation “revealed clear flow redistribution with a phase lag” because of fluid inertia. Numerous studies have measured fluid stiffness and damping from which the time delay could be inferred e.g. Tanaka & Takahara (11), Chen & Srikantiah (12) and Meskell & Fitzpatrick(13). More recently, Mahon & Meskell (14) measured the time delay between tube motion and a point in the flow located near the oscillating cylinder.

The governing equation of motion for a single degree freedom cylinder, oscillating in the direction normal to the mean flow only, is;

$$M_s\ddot{y} + c_s\dot{y} + k_s y = E(y, \dot{y}, \ddot{y}, U) \tag{1}$$

where E is the dynamic fluidelastic force acting on the tube. Eqn. 1 assumes the effects of vortex shedding and turbulent buffeting are ignored, which is not strictly correct but sufficient for a simplified approach. The detail of the function on the right is still unknown and it is here that the time delay is encountered. However, there are a number of models available in the literature for it (for an excellent overview, see the review of models by Price (2)). Many of the models decompose E into a number of fluid force coefficients. Hence, the fluidelastic behaviour of a single flexible cylinder could be characterised by two fluid forces (lift and drag). It is also apparent that the inclusion of a time delay or phase lag is a prerequisite for the models developed, as without the time delay the phenomenon cannot be modelled. The uncertainty as to the origin of the time delay is borne out by the different physical mechanisms for the inclusion of a time delay or phase lag in the models to predict fluidelastic instability. The three theoretical frameworks are: the “wavy-wall” model (Lever & Weaver (15)); the quasi-static model (Connors (16)); and the quasi-steady model (Price & Paidoussis (6)). There are also a number of empirical models. In addition, there have been a number of numerical simulations of fluidelastic instability using Large Eddy Simulation, Reynolds Averaged Navier Stokes and vortex methods.

Andjelic & Popp (17) have shown the importance of including a time delay in the model and compared their experimental data with the “wavy wall channel model” developed by Lever & Weaver (15). The time delay proposed in the Lever & Weaver model was obtained from various geometric length scales associated with the array geometry. However, Andjelic & Popp found that the fit between this approach and their experimental data was poor, but by dramatically modifying the time delay, they obtained a much better fit.

While the various models embed different flow physics, the critical velocity obtained also shows considerable sensitivity to the time delay value. Notwithstanding the central role that the

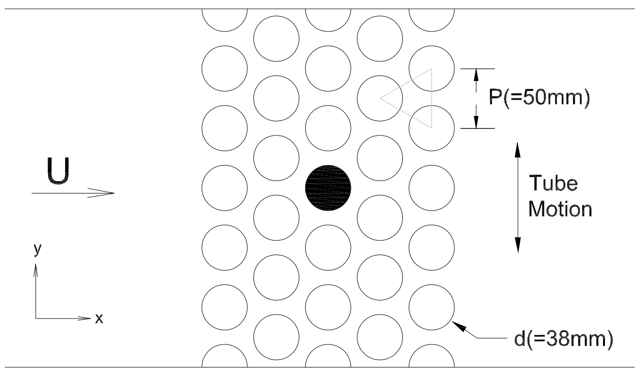

FIGURE 1. TEST SECTION SCHEMATIC.

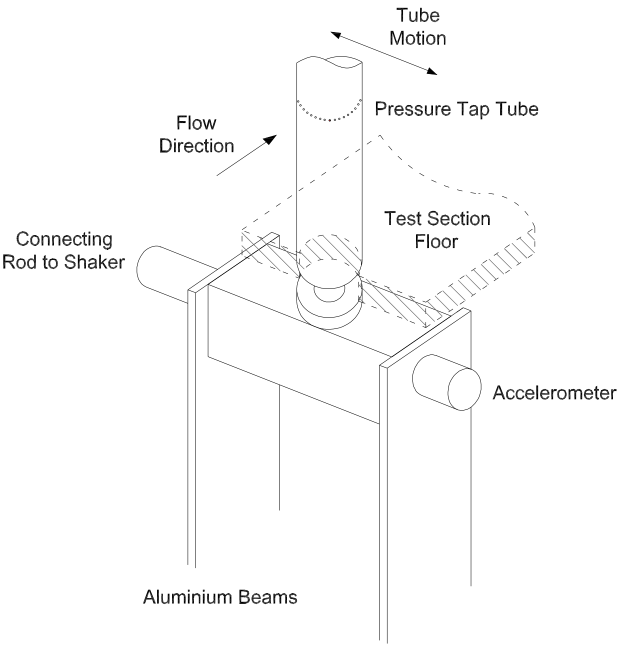

FIGURE 2. FLEXIBLE TUBE

time delay has in damping controlled fluidelastic phenomenon, there is very little direct evidence in tube arrays for the magnitude of this quantity. Estimates that do exist are inferred from the structural response. In this paper, the time delay between the fluid forces and the tube motion has been measured by directly monitoring the fluid force, rather than the result of the fluid force (i.e. the structural motion).

EXPERIMENTAL SETUP

Tests were carried out in a draw down wind tunnel with a velocity range from 2 m/s to 10 m/s with a free stream turbulence intensity of less than 1%. The flow velocity was measured using a Pitôt-static tube coupled with a micromanometer installed upstream of the test section. A five row normal triangular array with pitch ratio of 1.32 was investigated in this study. The tubes in the array are rigidly fixed, except for one tube which will be referred to as the instrumented cylinder (shaded cylinder, Fig. 1). The instrumented cylinder is rigid in construction, however, it is mounted on a flexible cantilevered support outside of the tunnel which is isolated from the wind tunnel test section. The tube was free to oscillate in the lift direction, y, only. A schematic illustrating the mounting scheme for the flexible tube is shown in Fig. 2. Also shown is a sectioned view of the test section floor through which the flexible tube was situated. The instrumented cylinder has 36 pressure taps with a diameter of 1 mm and located at the mid-span around the circumference of the cylinder (equispaced at 10^o intervals). The length of the cylinder assembly within the test section was 299 mm with a diameter of 38 mm.

The instrumented tube was connected to the pressure transducers with short lengths of 2 mm internal diameter silicone tubing. Each pressure tap was monitored with a differential pressure transducer (Honeywell 164PC01D37). The other port of the pressure transducer was vented to atmosphere. In effect the gauge pressure was measured. Further details on the instrumented tube can be found in Mahon (18) and Mahon & Meskell (19).

The tube oscillation was achieved using LDS V400 shaker connected to the flexible support via a rigid connecting rod. The input signal was generated using a HP35665A dynamic signal analyzer and was amplified using a LDS PA500 amplifier. The tube oscillation was measured using a PCB quartz shear accelerometer with a useful range of 0.2 - 7000 Hz (based on a maximum 5% variation in sensitivity). The accelerometer was mounted on the tube support as shown in Fig. 2.

The readings from the signal generator, accelerometer and pressure transducers were digitised and logged using an NI 48 channel, 24 bit data acquisition frame. Each channel was simultaneously sampled and automatically low pass filtered to avoid aliasing. Additional information on the test setup including schematics and photographs of the pressure tap tube can be found in Mahon (18).

The experimental setup has been validated previously (19) by measuring the mean pressure distribution around an isolated cylinder and comparing the results with those in the literature. The curve compares well with data in the literature e.g. Zukauskas (20). From the viewpoint of calibration, as no fluctuating measurements or high frequency sample rates were used only a simple calibration procedure was necessary. A known force was applied to a pressure transducer. From this, the sensitivity of the pressure transducer was obtained. However, in the current study fluctuating measurements were required hence, the calibration procedure is more complex and is discussed below.

System Calibration

In the current study, unsteady pressure measurements were acquired at a sample frequency of 2kHz. Hence, the calibration of the system is more complex as the properties to be determined when calibrating a pressure transducer are sensitivity, amplitude as a function of frequency, phase as a function of frequency, resonant frequency, damping ratio, rise time and overshoot. Furthermore, in the current setup there is also an additional time lag due to the pneumatic channel. For the fluctuating pressure measurements, the inherent time delay in the system (pressure transducer and pneumatic channel) needed to be quantified. The time lag in the pneumatic channel was due to the time taken for the pressure fluctuation to travel from the pressure tap on the surface of the instrumented cylinder via 1mm internal diameter brass tubing, expanded to 2mm silicone tubing connected to the pressure transducer.

The time delay was quantified by measuring the delay between a high quality GRAS microphone and system channel (pneumatic channel and pressure transducer). The calibration test setup requires that both the microphone and the pressure tap experience the same fluctuating pressures at all frequencies. This was achieved using the concept that in a cylindrical duct, only plane waves propagate below a certain cut-off frequency

$$f_{cut-off} = \frac{1.84c_{sp}}{2\pi a} \simeq 4kHz \tag{2}$$

where c_{sp} is the speed of sound and a is radius of the duct. In the current study the cut-off frequency was ~4kHz. If the instruments are located in the same plane along the duct they are exposed to the same pressure wave distribution for frequencies below the cut-off frequency. The calibration setup consisted of having the microphone and the pressure tap flush mounted at the end of an impedance tube. At the other end of the impedance tube a speaker connected to a signal generator. The system channel was calibrated against a high quality GRAS microphone to determine the inherent time delay in the system channel. Each channel was calibrated for 4.3, 6.6, 8.6 and 10.6Hz. Theses frequencies were chosen as they were the tube excitation frequencies under test in this study.

It was found that the time delay in the pneumatic channel was approximately 6.5-7ms and this was observed for all the excitation frequencies under test. However, there was an additional time delay due to the pressure transducer response and this was found to be frequency dependant. The time delay due to the pressure transducer response increased as the frequency reduced. Table. 1 shows the overall time delay for the excitation frequencies under test. These values were found to be similar for all 36 channels. The inherent delay in the pneumatic and pressure transducer responses was accounted for and removed. Hence, when the behaviour between the surface pressure and the tube motion is analyzed the time delay backed out is due to fluid reorganisation as a result of tube motion.

TABLE 1. System time delay

Frequency (Hz)	Time Delay (ms)
4.3	22
6.6	12
8.6	10
10.6	9

RESULTS

When fluidelastic instability is discussed in the literature, a time delay between the tube motion and the resulting fluid forces is postulated to be at the root of fluidelastic instability. The exact nature of the time delay is unclear and has yet to be measured directly. Granger & Paidoussis (8) indirectly measured the cause of the time delay using experimental data and a quasi-unsteady model. More recently Mahon & Meskell (14) measured a time delay between tube motion and a point in the flow located near the oscillating cylinder. In an ideal setup a time delay between tube motion and fluid forces would be measured. This was not achievable due to limitations in the setup. The justification for the approach above stems from the fact that the fluid forces on the cylinder are as a direct consequence of what is happening in the flow around the cylinder. Hence a relationship between the fluid flow and fluid forces are closely related. It would therefore seem reasonable to measure the response of the fluid instead of the fluid force as a first attempt to measure the time delay.

In the current study the test setup was modified so that the time delay between tube motion and fluid forces could be measured. This was achieved by measuring the surface pressure on the cylinder (See Fig. 3 for a schematic of tube angular position). The fluid forces were obtained by decomposing surface pressure into force contributions in the lift and drag directions and integrating these around the surface of the cylinder. The lift and drag forces are obtained directly from the surface pressure

$$F_L = -\int_0^{2\pi} Pdl\sin(\theta)d\theta \tag{3}$$

$$F_D = -\int_0^{2\pi} Pdl\cos(\theta)d\theta \tag{4}$$

In previous studies the authors have presented results on the static tube displacement (lift direction, y) of a cylinder within

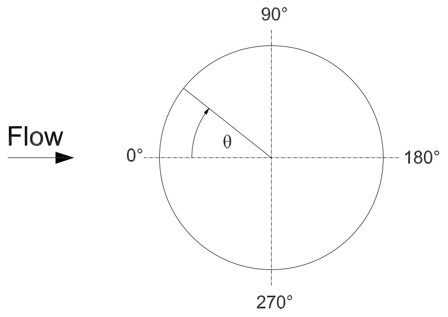

FIGURE 3. SCHEMATIC OF POSITION ANGLE

an array. It was observed that affect of tube displacement on the drag force was small with the drag force increasing with increasing tube displacement and Reynolds number. The maximum change in drag force of approximately 10% occurred at the largest tube displacement (y/d=10%) and Reynolds number (1.116×10^5) tested. The lift force around the cylinder was very well behaved fluctuating around zero when the tube was undisplaced (y/d=0%). When the tube was displaced, a net lift force in the direction opposite to the tube displacement results. The magnitude of the force generally increased with tube displacement and increasing flow velocity. In fact, the lift force increases from $\sim$0.5N to $\sim$3N, when the tube was displaced from y/d = 1% to y/d = 10%. From a physical viewpoint, the drag force was largely dependent on the bulk pressure drop across the array while the lift force was determined by local flow conditions. Hence, in the current study, the time delay between tube motion an fluid forces is restricted to the lift force only as the drag force does not change sufficiently with tube motion to accurately measure a time delay.

Time delay

The flexible cylinder was forced to oscillate at its natural frequency. The natural frequency of the system was modified by using different thickness beams for the twin beam support. The natural frequencies under test were 4.3, 6.6, 8.6 and 10.6Hz. The tube oscillation was achieved using a LDS shaker. The tube motion is measured using an accelerometer mounted on the twin beam support. From the tube acceleration data, an estimate of the tube displacement was extracted. This approach is valid as the tube oscillation was dominated by a single frequency. The excited vibration peak amplitudes chosen were 1, 2, 2.5 and 3% of the tube diameter (RMS level of 0.7, 1.17, 1.48 and 1.83%, respectively). Tests were conducted for seventeen free stream flow velocities ranging from 2-10m/s at 0.5m/s increments. Each test was conducted for 20 seconds at a sample rate of 2048Hz. At the lowest excitation frequency of 4.3Hz this translates to 86 averages thus improving the signal-to-noise ratio by a factor of 9.3.

Analysis technique A number of approaches were explored to extract the time delay between the tube response and the fluid forces. The first approach used the cross-spectrum between the tube response and the fluid force signal to extract the time delay. However, this approach was limited due to the relatively poor frequency resolution that could be obtained given the test parameters. The cross-correlation between the two signals was also attempted, providing improved temporal resolution. However, due to the high level of the random component due to turbulence, the narrow band process due to vortex shedding and the deterministic element due to the acoustic excitation, it was found that this approach did not yield satisfactory results. These problems could conceivably be overcome using a much longer record length, but this is impractical.

As an alternative, the data which are dominated by low frequency components are modelled as a short series of sinusoids in the time domain. The analysis technique employed for measuring the time delay was the same as that used in Mahon & Meskell (14). This offers the benefits of Fourier analysis (i.e. averaging) with the high temporal resolution achievable with a cross-correlation. For each test, tube motion, surface pressure and/or fluid force and the output signal from the amplifier (input signal to shaker) was acquired. The signal from the amplifier was used as a reference in the analysis as it produced a clean sinusoid whereas the surface pressure and tube response measurements include a random component as both were subject to turbulence in the flow. The reference signal was differentiated using a central difference method. Using the original and differentiated signals, the reference signal could be presented in terms of angular position. This enabled the tube motion and fluid forces to be related to angular position.

Fitting a harmonic curve to the data removes features from the flow field. However, the phenomenon of concern in the analysis is fluidelastic instability which is dominated by a low frequency sinusoidal response. It is understood that other flow features such as turbulence and vortex shedding exist but are not of concern in this analysis. As fluidelastic instability was phenomenon of interest in this case and was dominated by harmonic motion, the underlying behaviour was extracted by fitting a series of harmonic sinusoids.

$$p_M = \sum_{M=5}^{M} (A_M \sin M\theta + B_M \cos M\theta) + c \qquad (5)$$

where p_M is the pressure, θ is the angular position of the reference signal, A_M and B_M are constants. The constants A_M and B_M were obtained using a pseudo-inverse method which yielded a least squares fit for an over determined set of equations (Keays & Meskell (21)).

The flow field around the cylinder in a tube array is highly sheared and at some positions it was clear that the surface pressure does not respond linearly to the tube motion. It is therefore important to consider how the quality of the fit was determined. This was determined using a number of criteria. The approach used in this study examined the energy contribution at each harmonic in conjunction with the auto-correlation between the actual data less the first harmonic fit. A good fit was deemed to have been achieved when the energy distribution at the first harmonic was greater than 95%. Below that threshold the fit was deemed to be not of the base line quality. The second criteria also had to be satisfied. This involved examining the auto-correlation of the raw data with the fit of the first harmonic removed. If the fit was good random noise should be all that remains. Viewing the auto-correlation of this signal determines if the resulting distribution was random or if it contained periodic artifacts.

As only the first harmonic is of interest, the data can be represented as;

$$p_1 = A_1 \sin\theta_1 + B_1 \cos\theta_1 + c \tag{6}$$

Plotting the normalised AC component of tube response and the fluid forces together clearly shows that there is a phase difference between the two. Specifically, the fluid force lags behind the tube response. Using the constants A_1 and B_1 the phase with respect to the reference signal for both fits can be obtained from the $tan^{-1}\frac{A_1}{B_1}$. Subtracting the phases between the two traces yields a phase difference, $\Delta\phi$. This was converted into a time delay, τ, as the excitation frequency is known:

$$\Delta\phi = \omega\tau \tag{7}$$

where $\omega = 2\pi f_n$, f_n is the excitation frequency.

As detailed above there was an inherent time lag in the system due to the pneumatic channel which consisted of the surface pressure tap, brass tubing and silicon tubing; and the response of the pressure transducer which was frequency dependant. A rigorous calibration procedure was implemented for the pressure channel. This enabled the time lag in this part of the measurement system to be quantified and removed. The latency in the tube response measurement has been quantified and removed using a test data and physical limitations of the flow, as will be described below. Hence, all the raw phase lag can be correct to yield the time delay between tube motion and the the resulting fluid forces at the root of fluid damping controlled instability.

Fig. 4 plots the time delay against velocity at a tube excitation frequency of 8.6Hz and for four levels of tube oscillation amplitude. There is some scatter in data but this is to be expected given the high turbulent and sheared nature of the flow in the tube array. In the main it is observed that the data collapses to a single curve indicating that the time delay is not dependent on the amplitude of oscillation. Similar results were observed for the other excitation frequencies tested. Given that it was shown that the time delay was independent of tube oscillation amplitude, the data at a given excitation frequency at all vibration amplitudes were collapsed on to a single plot and averaged. Fig. 5 plots the time delay against velocity for excitation frequencies of 6.6, 8.6 and 10.6Hz. It is observed that the time delay reduces with increasing velocity. This was generally found to be the case at all excitation frequencies tested except 4.3Hz. It is thought that poor signal-to-noise ratio affected the results at this frequency. For the reason outlined above, any further analysis on the data will omit the results from the 4.3Hz excitation tests.

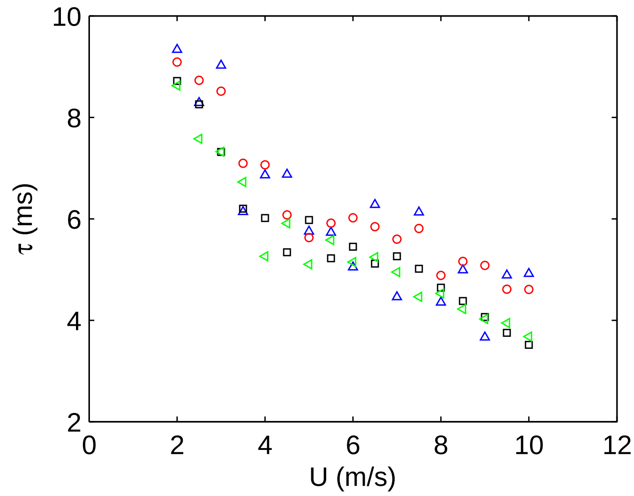

FIGURE 4. TIME DELAY AGAINST VELOCITY AT A TUBE EXCITATION FREQUENCY OF 8.6HZ. PEAK AMPLITUDES; △, 1%; ○, 2%; □, 2.5% ◁ – 3%

Plotting (Fig. 6) the time delay against convection time (d/U) for three excitation frequencies (6.6, 8.6 and 10.6Hz) and all four tube oscillation amplitudes. In general it is observed that the time delay reduces with increasing convection velocity and the data follows a definite trend. However, there is some scatter with the main source of scatter occurring at the excitation frequency of 6.6Hz. This probably due to the poorer signal-to-noise ratio at this excitation frequency. The overall trend was one of a reducing time delay as d/U decreases.

Assuming, as is almost universally accepted, that the fluidelastic time delay is due to a convection process, then physically, at zero convection time (i.e. an infinite convection speed) the time delay must be zero. In order to assess the offset in the measurement system it is assumed that the time delay responses linearly with convection time. Hence, in order to assess the offset in the measurement system, a single straight line is fitted, and intercepts the y-axis at approximately 3ms. This is the system offset, ε.

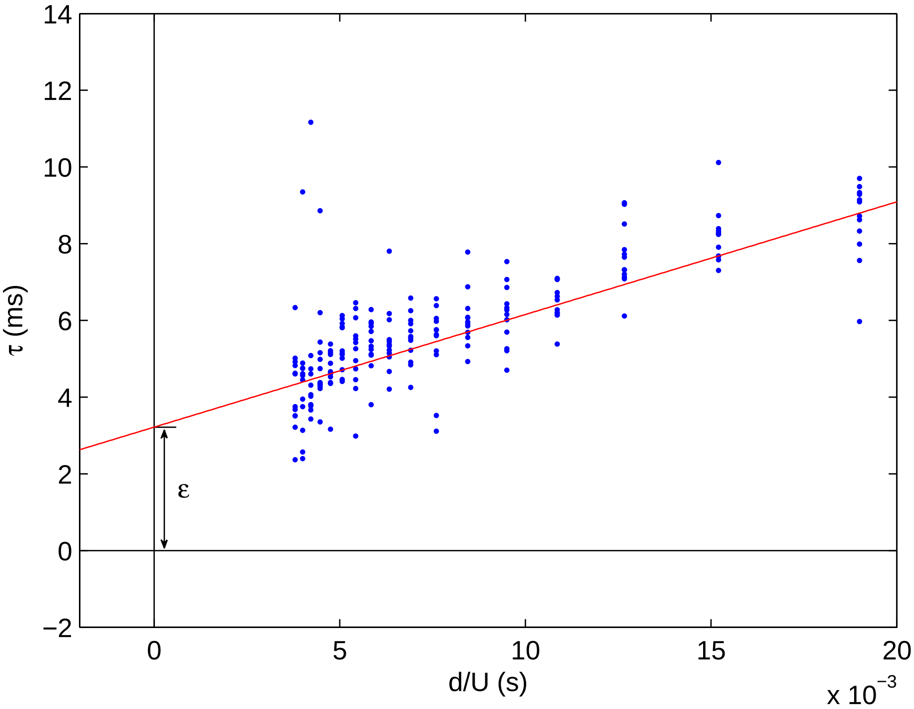

FIGURE 6. TIME DELAY AGAINST CONVECTION TIME AT EXCITATION FREQUENCIES OF 6.6, 8.6 AND 10.6HZ AND AMPLITUDES OF 1, 2, 2.5 AND 3%: •, EXPERIMENTAL DATA; –, BEST FIT LINE

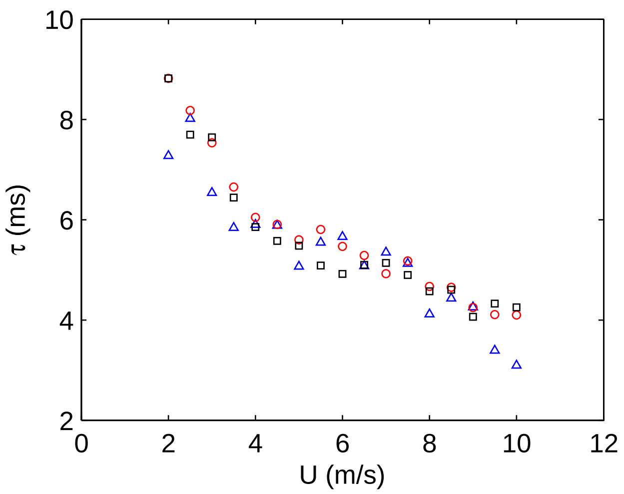

FIGURE 5. UNCORRECTED TIME DELAY AT VARIOUS TUBE EXCITATION FREQUENCIES; △, 6.6HZ; ○, 8.6HZ; □, 10.6HZ

The tests were repeated a number of times and repeated for different tube orientations (i.e. pressure tap 1 at the front of the cylinder (θ=0^o) was rotated so that pressure tap 1 was at (θ=90^o)) to quantify if there was a bias in the setup. However, the results from the repeated tests were all in excellent agreement. As it was established that repeating the tests resulted in a similar outcome, the system offset was attributed to a systemic error in the tube response measurement. Nonetheless, the system offset was accounted for and the data corrected by subtracting ε.

The corrected time delay is non-dimensionaled by multiplying it by the frequency, τ_1=τf. Fig. 7 plots the non-dimensional time delay against reduced velocity (U_r=U/fd). The data collapses onto a single curve. There is some scatter in the data but this is not surprising given that the time delay has been obtained from a measurement in a tube array were the flow is highly sheared and turbulent. As the data collapses to a single curve, this would imply that the time delay is independent of the tube excitation frequency for the frequency range under investigation in this study. Higher excitation frequencies should also be examined to rigorously evaluate this observation but this was not possible with the current setup.

In Fig. 8 the corrected time delay is non-dimensionalised by multiplying by velocity and dividing by tube diameter, τ_2=τU/d is plot against Reynolds number. The non-dimensionalised time delay, τ_2 collapses about a constant of 0.29. The significance of the constant will be discussed below.

Fig. 9 shows the corrected time delay (τ) against velocity.

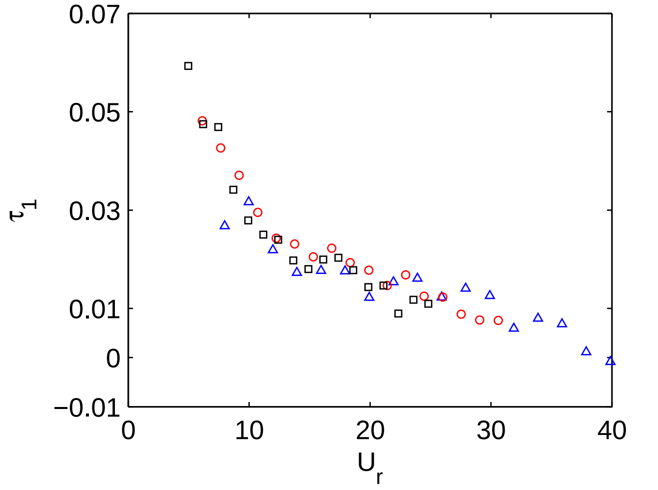

FIGURE 7. NON-DIMENSIONAL TIME DELAY (τ_1) AGAINST REDUCED VELOCITY AT VARIOUS TUBE EXCITATION FREQUENCIES; △, 6.6HZ; ○, 8.6HZ; □, 10.6HZ

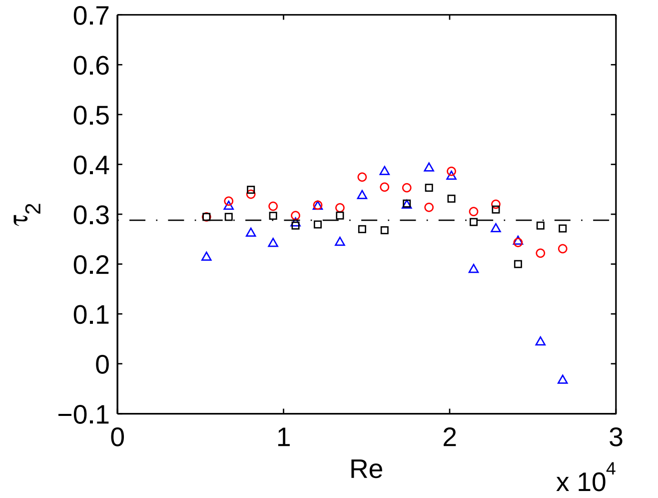

FIGURE 8. NON-DIMENSIONAL TIME DELAY (τ_2) AGAINST REYNOLDS NUMBER AT VARIOUS TUBE EXCITATION FREQUENCIES; △, 6.6HZ; ○, 8.6HZ; □, 10.6HZ

The data collapses well onto a single curve. It is also observed that the time delay reduces with increasing flow velocity. These results are in qualitative agreement with of the time delay proposed by Price & Paidoussis ($\tau = \mu d/U$). Price & Paidoussis suggest that $\mu \sim O(1)$, if this value is used the time delay is significantly larger than experimental data. In Fig. 9 the time delay proposed by Price & Paidoussis is plot. However, the authors choose $\mu \sim O(0.29)$ rather than $O(1)$. The value for μ was obtained from Fig. 8. Using this value for μ in Price & Paidoussis expression results in excellent quantitative agreement between theory and the experimental data. The difference in the values of μ may indicate that μ is a geometry dependant quantity which is not unreasonable as gap velocity, inter-cylinder spacing and general fluid flow behaviour is highly dependant on the array geometry. However, further work is required to test this hypothesis as only the time delay for a single array has been measured.

It has been shown above that the time delay between tube motion and the resulting fluid forces reduces as flow velocity increases. However, examining the time delay at each individual pressure tap it is apparent that the response between tube motion and the pressure signal is not linear at positions at the front of the cylinder and rear of the cylinder this is due to a number of reasons. Firstly the positions are generally in the normal direction to tube motion. Secondly, examining the mean pressure distribution (Fig. 10) it is apparent that certain angular positions like the front stagnation point and the region at the rear of the cylinder (150-210^o) do not show large changes in the lift force due to the tube displacement. Hence, it is difficult to quantify a time delay in these regions.

Fig. 11 shows the time delay between tube motion and the resulting pressure field on one side of the cylinder (220-350^o). The opposite side of the cylinder behaves in a similar manner. In general it is observed that the time lag reduces with increasing flow velocity which is in agreement with the analysis above. However, at some locations (300-320^o) it is observed that the opposite trend occurs. Examining Fig. 12, the rms of the pressure signal at the excitation frequency was normalised with respect to the rms pressure at θ=0^o and plot against tube angular position. It is observed that the amplitude of oscillation in the pressure signal (due to tube motion) at θ=300-320^o is high. Hence, the reverse trend in the time delay experienced at these position angles is real and is not an artifact of a weak data set. Hence, the change in trend is due to fluid behaviour in those regions. It is not clear why this is the case. However, examining the static tube displacement (Fig. 10) the region where the time delay behaviour differs to what is generally understood behaviour postulated in the literature is the same region where the knuckle develops in Fig. 10. If one considers that the time delay is a function of velocity and tube diameter as proposed by Price & Paidoussis this would imply that the increase in time delay (300-320^o) is due to a reduction in flow velocity in this region.

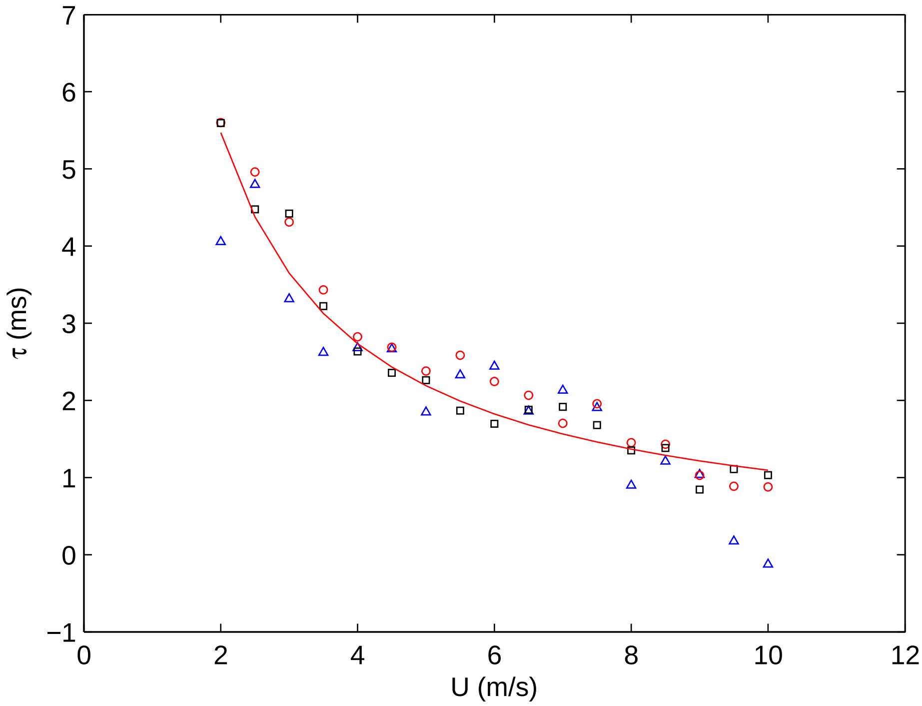

FIGURE 9. TIME DELAY AGAINST VELOCITY AT VARIOUS TUBE EXCITATION FREQUENCIES; △, 6.6HZ; ○, 8.6HZ; ⋄, 10.6HZ. –, PRICE & PAIDOUSSIS MODEL (μ=0.29)

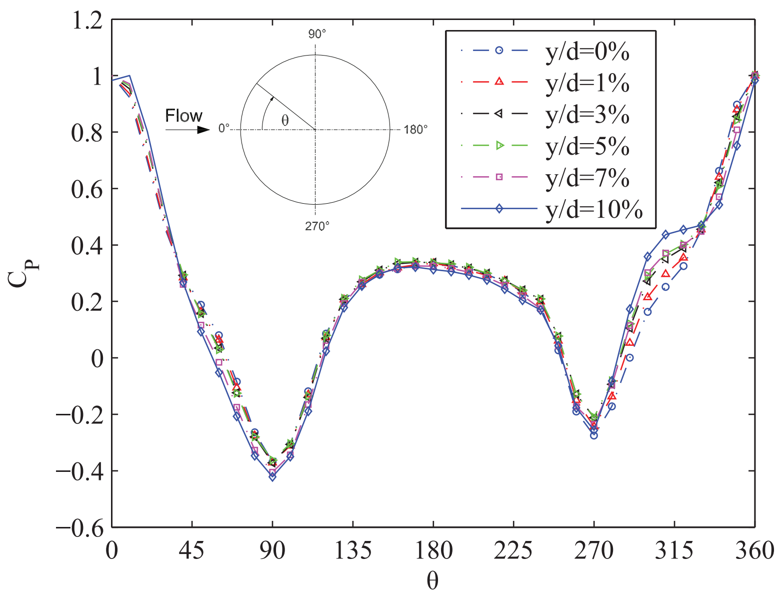

FIGURE 10. P/d=1.32; C_P AT VARIOUS TUBE DISPLACEMENTS, U=7 m/s (Re=7.82×10^4)

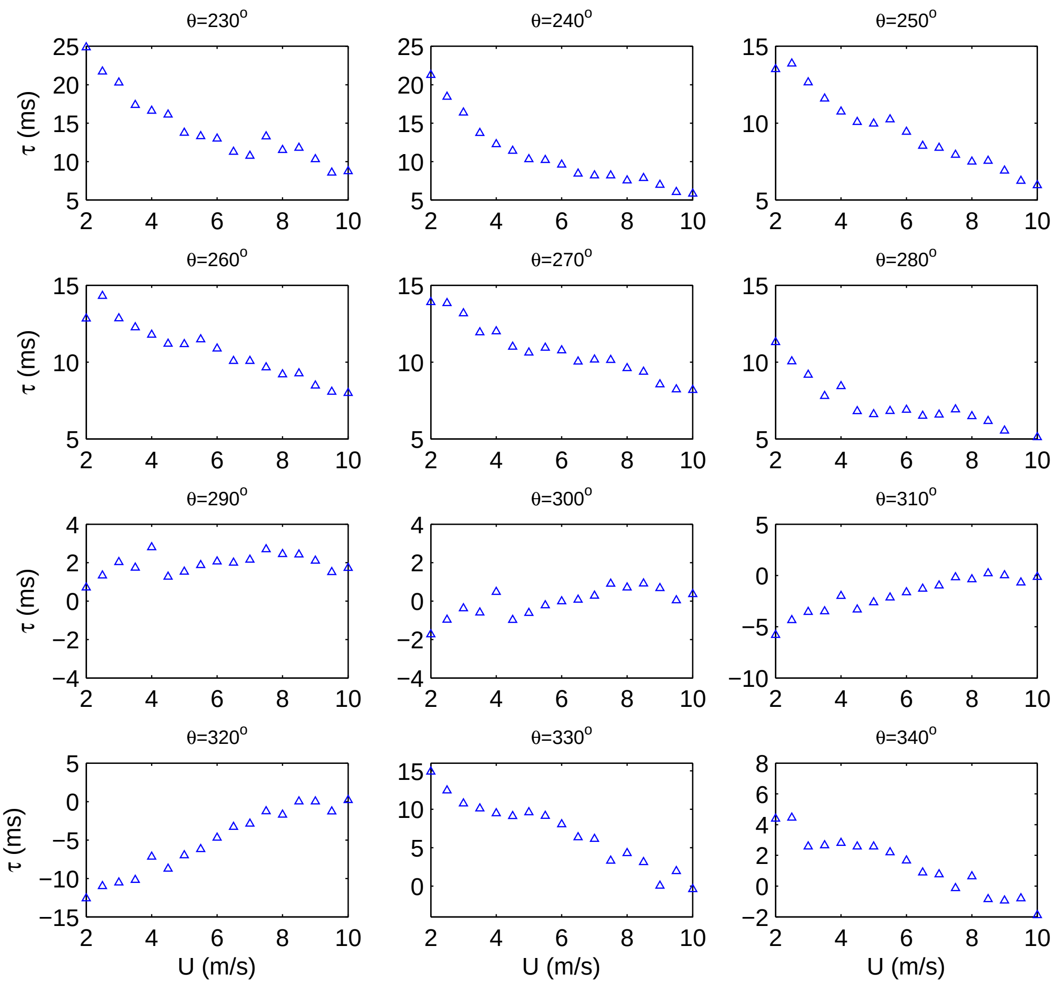

FIGURE 11. TIME DELAY AT AN EXCITATION FREQUENCY OF 10.6HZ FOR VARIOUS POSITION ANGLES

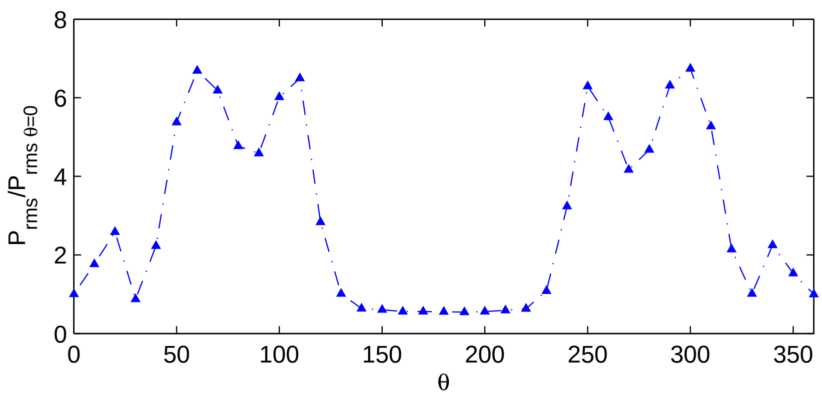

FIGURE 12. NORMALISED RMS PRESSURE AT AN EXCITATION FREQUENCY OF 10.6HZ AGAINST POSITION ANGLE

CONCLUSIONS

It is generally understood that there is a time delay between tube motion and the resulting fluid forces at the root of fluid damping controlled instability. The exact nature of the time delay is still unclear. The current study has directly measured the time delay between tube motion and the resulting fluid forces in a normal triangular tube array with a pitch ratio of 1.32 with air cross-flow. The non-dimensional time delay measured was constant over the velocity range tested, and was independent of frequency and tube vibration amplitude. The value of the time delay was of the order of magnitude assumed in the semi-empirical models of by Price & Paidoussis (6), Weaver *et al.* (15), Granger & Paidoussis (8) and Meskell (9). Specifically, the time delay is 0.3. Although, further work is required to provide a parameterized model of the time delay which can be embedded in the various models, the data already provides some insight into the physical mechanism responsible.

ACKNOWLEDGMENT

This publication has emanated from research conducted with the financial support of Science Foundation Ireland.

REFERENCES

[1] Adobes, A., Pillet, J., David, F., and Gaudin, M., 2006. "Influence of steam generator tube bundle vibrations on the operating diagram of a nuclear plant during strech out". *ASME PVP, Flow Induced Vibrations,* ***ICPVT-11***(93239), pp. 1–10.

[2] Price, S. J., 1995. "A review of theoretical models for fluidelastic instability of cylinder arrays in cross-flow". *Journal of Fluids and Structures,* ***9***, pp. 463–518.

[3] Paidoussis, M. P., and Price, S., 1988. "The mechanisms underlying flow-induced instabilities of cylindre arrays in crossflow". *Journal of Fluid Mechanics,* ***187***, pp. 45–59.

[4] Chen, S. S., 1983. "Instability mechanisms and stability criteria of a group of circular cylinders subjected to cross-flow. part i: Theory". *ASME Journal of Vibrations, Acoustics, Stress, Reliability and Design,* ***105***, pp. 51–58.

[5] Chen, S. S., 1983. "Instability mechanisms and stability criteria of a group of circular cylinders subjected to cross-flow. part ii: Numerical results and discussion". *ASME Journal of Vibrations, Acoustics, Stress, Reliability and Design,* ***105***, pp. 253–260.

[6] Price, S. J., and Paidoussis, M. P., 1984. "An improved mathematical model for the stability of cylinder rows subject to cross-flow". *Journal of Sound and Vibration,* ***97***(4), pp. 615–640.

[7] Price, S. J., and Kuran, S., 1991. "Fluidelastic stability of a rotated square array with multiple flexible cylinders, subject to cross-flow". *Journal of Fluids and Structures,* ***5***, pp. 551–572.

[8] Granger, S., and Paidoussis, M., 1996. "An improvement to the quasi-steady model with application to cross-flow-induced vibration of tube arrays". *Journal of Fluid Mechanics,* ***320***, pp. 163–184.

[9] Meskell, C., 2009. "A new model for damping controlled fluidelastic instability in heat exchanger tube arrays". *Journal Proceedings of the Institution of Mechanical Engineers, Part A: Journal of Power and Energy,* ***223***(4), pp. 361–368.

[10] Abd-Rabbo, A., and Weaver, D. S., 1986. "A flow visualisation study of flow development in a staggered tube array". *Journal of Sound and Vibration,* ***106***(2), pp. 241–256.

[11] Tanaka, H., and Takahara, S., 1981. "Fluid elastic vibration of tube array in cross flow". *Journal of Sound and Vibration,* ***77***(1), pp. 19–37.

[12] Chen, S. S., and Srikantiah, G. S., 2001. "Motion-dependent fluid force coefficients for tubes arrays in cross-flow". *ASME Journal of Pressure Vessel Technology,* ***123***, pp. 429–436.

[13] Meskell, C., and Fitzpatrick, J. A., 2003. "Investigation of the nonlinear behaviour of damping controlled fluidelastic instability in a normal triangular tube array". *Journal of Fluids and Structures,* ***18***, pp. 573–593.

[14] Mahon, J., and Meskell, C., 2009. "Investigation of the underlying cause of the interaction between acoustic resonance and fluidelastic instability in normal triangular tube arrays". *Journal of Sound and Vibration,* ***324***, pp. 91–106.

[15] Lever, J., and Weaver, D., 1986. "On the stability of heat exchanger tube bundles. part i: modified theoretical model. part ii: numerical results and comparison with experiment". *Journal of Sound and Vibration,* ***107***, pp. 375–410.

[16] Connors, H. J., 1970. "Fluid-elastic vibration of tube arrays excited by cross flow". *Proceedings, Flow-induced vibrations in heat exchangers, ASME, Chicago*, pp. 42–56.

[17] Andjelic, M., and Popp, K., 1989. "Stability effects in a normal triangular cylinder array". *Journal of Fluids and Structures,* ***3***(2), pp. 165–185.

[18] Mahon, J., 2008. "Interaction between acoustic resonance and fluidelastic instability in a normal triangular tube arrays". PhD thesis, Trinity College Dublin.

[19] Mahon, J., and Meskell, C., 2009. "Surface pressure distribution survey in normal triangular tube arrays". *Journal of Fluids and Structures,* ***25***, pp. 1348–1368.

[20] Zukauskas, A., 1989. "Cylinders in crosflow". *High-Performance Single-Phase Heat Exchangers, Hemisphere Publishing Corporation,* **Chapter 10**, pp. 187–206.

[21] Keays, J., and Meskell, C., 2006. "A study of the behaviour of a single-bladed waste-water pump". *Journal of Process Mechanical Engineering,* ***220***(2), pp. 79–87.